



Published in final edited form as:

Biochem Pharmacol. 2015 October 15; 97(4): 566–575. doi:10.1016/j.bcp.2015.07.030.

Development of [¹⁸F]ASEM, a specific radiotracer for quantification of the α7-nAChR with positron-emission tomography

A.G. Horti

Department of Radiology, The Johns Hopkins School of Medicine, 600 North Wolfe Street, Baltimore, MD 21287-0816, USA

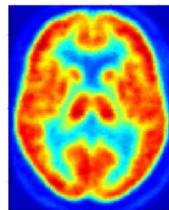
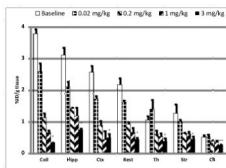
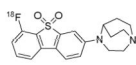
Abstract

The alpha-7 subtype of the nicotinic acetylcholine receptor (α7-nAChR) is fundamental to physiology; it mediates various brain functions and represents an important target for drug discovery. Exploration of the brain nicotinic acetylcholine receptors (nAChRs) using positron-emission tomography (PET) will make it possible to better understand the important role of this receptor and to study its involvement in schizophrenia, bipolar disorder, Alzheimer's and Parkinson's diseases, drug dependence, inflammation and many other disorders and simplify the development of nicotinic drugs for treatment of these disorders.

Until recently, PET imaging of α7-nAChRs has been impeded by the absence of good radiotracers. This review describes various endeavors to develop α7-nAChR PET tracers by several research groups including the author's group. Most initial PET tracers for imaging α7-nAChRs did not exhibit suitable imaging properties due to their low specific binding. Recently discovered [¹⁸F]ASEM is the first highly specific α7-nAChR radioligand and it was recently translated to human PET imaging.

Abstract

¹⁸F]ASEM



Corresponding author: Andrew G. Horti, PhD, PET Center, Division of Nuclear Medicine, Radiology, Johns Hopkins Medicine, 600 North Wolfe Street, Nelson B1-122, Baltimore, MD 21287-0816 USA, Phone: 410-614-5130, Fax: 410-614-0111, ahorti1@jhmi.edu.

Publisher's Disclaimer: This is a PDF file of an unedited manuscript that has been accepted for publication. As a service to our customers we are providing this early version of the manuscript. The manuscript will undergo copyediting, typesetting, and review of the resulting proof before it is published in its final citable form. Please note that during the production process errors may be discovered which could affect the content, and all legal disclaimers that apply to the journal pertain.

Keywords

positron emission tomography; PET; $\alpha 7$ -nAChR; alpha 7; nicotinic receptor; [^{18}F]ASEM

1. Introduction

Nicotinic cholinergic receptors (nAChRs) are neurotransmitter-gated cationic channels that are present in the central nervous system (CNS), autonomic and sensory ganglia, and various non-neuronal cells. Two nAChR subtypes, $\alpha 4\beta 2$ - and $\alpha 7$ -nAChR, are the most abundant nAChRs in the CNS[1].

The $\alpha 7$ -nAChR subtype is highly expressed in the human brain and this subtype has been implicated in the pathophysiology of a variety of brain disorders and conditions including schizophrenia, Alzheimer's disease, bipolar disorder, traumatic brain injury, anxiety, depression, multiple sclerosis, inflammation, and drug addiction[1-10].

As was demonstrated in post-mortem studies, the density of $\alpha 7$ -nAChRs in human brain tissue is significantly altered in many disorders:

Schizophrenia

In autoradiography and immunochemistry studies, Freedman *et al*[11] and others [12-17] have demonstrated a significant post-mortem reduction (25-54%) of $\alpha 7$ -nAChR binding or expression in the hippocampus and cortex of subjects with schizophrenia *vs.* controls.

Alzheimer's disease

A characteristic of Alzheimer's disease is degeneration of cholinergic neurons[18]. A number of reports have described a significant loss of $\alpha 7$ -nAChRs in the cortex and hippocampus of patients with Alzheimer's disease [15, 19] (see also review[20]).

Bipolar disorder

An autoradiography study using an $\alpha 7$ -nAChR radiotracer demonstrated an increased binding in the hippocampus and perirhinal cortex in the brain slices of the subjects suffering from bipolar disorder[21].

Traumatic brain injury

Traumatic brain injury is a significant public health problem with almost 2 million documented cases per year in the USA, with a mortality of 20%[22, 23]. Several reports found a significant reduction (30-70%, *ex vivo* or *in vitro*) of $\alpha 7$ -nAChRs in animal models of traumatic brain injury [8, 24-26], suggesting that alteration of the $\alpha 7$ -nAChR is a crucial component of the biochemical perturbation caused by traumatic brain injury.

The difference in the density of $\alpha 7$ -nAChRs in the brain between healthy subjects and patients suffering from various disorders was quantified in post-mortem studies, but it never was observed in the living human brain. Non-invasive quantification of $\alpha 7$ -nAChRs in humans would provide a better understanding of their role in various CNS disorders and

could also simplify the development of nicotinic drugs for treatment of these disorders [27-32].

PET provides the best opportunity for quantification of receptors in the human brain – better than any other clinical imaging modality [33, 34]. However, since the invention of the PET technique in 1975 fewer than 40 of the existing receptors in the human brain have been imaged due to the lack of available PET radiotracers (see <http://www.nimh.nih.gov/research-priorities/therapeutics/cns-radiotracer-table.shtml>). Until recently, one of the major cerebral receptors lacking an appropriate PET radioligand for human imaging was $\alpha 7$ -nAChR. The recently developed PET radioligand [^{18}F]ASEM has opened new avenues in noninvasive imaging of this receptor system in human subjects.

2. Initial PET radioligands for $\alpha 7$ -nAChRs

In principle, a quality $\alpha 7$ -nAChR radioligand for PET should exhibit the same set of characteristics as PET tracers for most other brain receptors: 1) a high specific and low non-specific binding in vivo; 2) high selectivity versus non-target binding sites; 3) reversible brain kinetics with good blood-brain barrier permeability; 4) radiochemistry that is suitable for short-lived isotopes; and 5) low radiation burden and toxicity. These general requirements for PET radiotracers have been summarized in many reviews [35-37].

While all general requirements must be met, the high specific binding is the most demanding property in the development of $\alpha 7$ -nAChR radiotracers. Specific PET tracers for brain receptors are expected to obey the Eckelman's criterion that $B_{\text{max}}/K_D \geq 10$ (B_{max} = binding site density; K_D = binding affinity constant of the radiotracer)[38, 39]. The concentration of the $\alpha 7$ -nAChR binding sites in the primate brain is low ($B_{\text{max}} = 5 - 15$ fmol/mg protein or $1.5 - 12$ fmol/mg tissue)[12, 40, 41]. Consequently, the expected binding affinity for a quality $\alpha 7$ -nAChR PET radioligand must be in a sub-nanomolar range. This binding affinity requirement challenged the development of suitable $\alpha 7$ -nAChR radioligands (see reviews[35, 42, 43]).

Investigators have been attempting to develop $\alpha 7$ -nAChR radioligands for in vivo imaging since the pioneering work of the Dolle[44] (Orsay, France) and Pomper[45] (Baltimore, US) in 2001-2005. Both groups radiolabeled quinuclidine derivatives (Fig. 1) that were previously reported by AstraZeneca as potential $\alpha 7$ -nAChR drugs. Unfortunately, these radiotracers did not exhibit a sufficient signal-to-noise ratio in lab animals and were not translated to humans.

In 2005-2010 many researchers, including our own group, worked on the development of a clinically viable $\alpha 7$ -nAChR PET radioligand, and about two dozen $\alpha 7$ -nAChR compounds were radiolabeled with [^{18}F] or [^{11}C]. As summarized in the recent reviews[35, 46-48], those efforts did not lead to an $\alpha 7$ -nAChR PET radioligand with sufficient in vivo specificity.

[^{11}C]CHIBA-1001 was the only $\alpha 7$ -nAChR radioligand translated to human PET in the past, but it showed low target-to-non-target ratios in the brain (<1.3) in a single human PET scan[49] (Fig. 2). Further blocking experiments using PET in humans demonstrated some

specificity of the [^{11}C]CHIBA-1001 binding that, however, was not sufficiently high for reliable receptor quantification. This result led [^{11}C]CHIBA-1001 inventors to a conclusion that a better PET radioligand is necessary[50]. The low specific binding of [^{11}C]CHIBA-1001 in the human brain is in agreement with its relatively low in vitro binding affinity ([^3H]CHIBA-1001, rat or human $K_D = 120 - 193 \text{ nM}$) and its inadequate $\alpha 7$ -nAChR regional distribution in the rodent brain[51, 52].

The most recent $\alpha 7$ -nAChR PET radioligands, [^{18}F]AZ11637326[53, 54], [^{11}C]NS14492[55] and [^{18}F]NS10743[56, 57] (Fig. 3), exhibited some specific binding in the brains of lab animals, but their specificities were also insufficient for human PET. The main reason for the deficient PET properties of most of the initial radioligands was due to the low binding affinity of these compounds (see for review[48]). Another recent PET tracer [^{11}C]A752274 (Fig. 3) that was developed by collaboration of Abbott Laboratories and Johns Hopkins University exhibited very high binding affinity ($K_i = 0.092 \text{ nM}$). Unfortunately, [^{11}C]A752274 is a polar compound with low lipophilicity ($\log D_{7.4} = -2.7$) that shows low brain uptake in animals, which makes it inappropriate for brain PET[58].

3. Development of [^{18}F]ASEM[48, 59]

3.1 Synthesis of ASEM

In 2012 Abbott Laboratories disclosed a number of $\alpha 7$ -nAChR ligands that were synthesized as potential drug candidates[60]. One of the compounds of the series was 3-(1,4-diazabicyclo[3.2.2]nonan-4-yl)dibenzo[*b,d*]thiophene 5,5-dioxide (Fig. 4), an $\alpha 7$ -nAChR selective ligand with exceptionally high binding affinity, $K_i = 0.023 \text{ nM}$, and the ability to penetrate the blood-brain barrier in lab animals[60]. These properties made this dibenzothiophene compound an attractive lead for development of quality $\alpha 7$ -nAChR PET tracers.

Even though the Abbott lead (Fig. 4) is difficult to radiolabel with the PET radionuclide ^{11}C , the presence of an electron-withdrawing sulfonyl group opened an opportunity for making [^{18}F]fluoro-derivatives of this compound via the nucleophilic aromatic substitution with [^{18}F]fluoride. PET chemists from JHU synthesized a series of fluoro-derivatives of 3-(1,4-diazabicyclo[3.2.2]nonan-4-yl)dibenzo[*b,d*]thiophene 5,5-dioxide. Within the series, 4-(6-fluorodibenzo[*b,d*]thiophen-3-yl)-1,4-diazabicyclo[3.2.2]nonane 5,5-dioxide (JHU82132, ASEM) and its *para*-isomer (JHU82108, *para*-ASEM) exhibited the best $\alpha 7$ -nAChR in vitro binding affinity and high selectivity vs. heteromeric nAChR subtypes or 5-HT $_3$ [48, 59] (see Table 1). The abbreviation “ASEM” stands for ALPHA-SEVEN (A-CEM β) in Greek-Russian as was suggested by Dr. R.F. Dannals from Johns Hopkins University.

Prior radiolabeling of [^{18}F]ASEM and further animal experiments the JHU group forecasted the PET imaging value of this compound by comparison of its in vitro binding affinity versus the previous best $\alpha 7$ -nAChR PET tracers [^{18}F]AZ11637326, [^{11}C]NS14492 and [^{18}F]NS10743(Fig. 3). The binding assay of all four compounds was performed under the same assay conditions (Table 2). This head-to-head comparison demonstrated that the $\alpha 7$ -nAChR affinity of ASEM is 1-2 orders of magnitude superior to the previous

radiotracers[48] and in vivo specific binding of [^{18}F]ASEM was expected to be proportionally greater.

In addition to the promising binding affinity, other molecular determinants of ASEM that are important for the blood-brain barrier permeability (molecular weight = 358; lipophilicity $\log D_{7.4} = 2.0$; polar surface area = 49) are within the optimal range for most brain PET tracers[61, 62].

The appropriate in vitro properties of ASEM for PET and its potential suitability for [^{18}F]-radiolabeling were the driving forces behind the radiosynthesis of [^{18}F]ASEM and further in vivo experiments with this radiotracer. The isomer *para*-ASEM was selected as a back-up compound since it manifested fairly comparable in vitro binding affinity properties as ASEM (Table 1).

3.2 Radiosynthesis of [^{18}F]ASEM and *para*-[^{18}F]ASEM

Among the main requirements for [^{18}F]-labeled (half-life $t_{1/2} = 109.77$ min) PET tracers is an efficient radiolabeling and its suitability for automation and preparation of the final product with high specific radioactivity, purity and radiochemical yield. The high specific radioactivity of PET radiotracers for neuroreceptors is a general requirement because of the concerns about the binding competition between the [^{18}F] radiotracer and its natural non-radioactive [^{19}F] isotopomer (carrier), which is always present in the radiolabeled product [63]. For reliable quantification analysis and also due to the safety concerns, a dose of PET radiotracer should occupy less than 5% of the available binding sites. This general requirement makes it necessary for a radiotracer to contain a low mass of carrier or, in other words, exhibit high specific radioactivity. Due to the low density of $\alpha 7$ -nAChRs in the brain (see above) the radiotracers for this receptor should be used for PET studies only at a specific radioactivity greater than 5000 – 10000 mCi/ μmol [35].

[^{18}F]ASEM and *para*-[^{18}F]ASEM were prepared by a Kryptofix-222[®] – assisted reaction of the corresponding nitro-precursors, PRE-ASEM and PRE-*para*-ASEM, with [^{18}F]fluoride (Fig. 5). The radiosynthesis was performed remotely in a PC-controlled radiochemistry synthesis module (Microlab, GE). The final radiolabeled products were purified by preparative high-performance liquid chromatography (HPLC) and solid-phase extraction and formulated as sterile apyrogenic solutions in 7% ethanolic saline. Both radiotracers, [^{18}F]ASEM and *para*-[^{18}F]ASEM, were prepared with comparable radiochemical yields of $16 \pm 6\%$ ($n=14$) (non-decay-corrected), specific radioactivities in the range of 330 - 1260 GBq/ μmol (9-34 Ci/ μmol), and a radiochemical purity greater than 99%[48].

With increased demand for the [^{18}F]ASEM for human and animal PET studies, a fast microwave-assisted synthesis with improved radiochemical yield (25-50%) was further developed[64]. The microwave method allows a routine preparation of about 500 mCi [^{18}F]ASEM per batch with high specific radioactivity (>10000 mCi/ μmol) and radiochemical purity ($>98\%$), which means that it can be used for several PET scans within the same day.

4. Pre-clinical studies with [¹⁸F]ASEM in mice

4.1 Biodistribution in CD1 mice

After the successful radiosynthesis of [¹⁸F]ASEM, the radiotracer biodistribution, in vivo binding specificity, selectivity and brain kinetics were evaluated in CD1 mice [48].

In the *ex vivo* biodistribution experiments each mouse received an injection of [¹⁸F]ASEM into a lateral tail vein [48]. The animals were sacrificed at certain time points (5 – 120 min) and the brain regions were quickly dissected and assayed in a gamma-counter and time-radioactivity curves (**Fig. 6**) were generated. The study demonstrated that [¹⁸F]ASEM readily entered the mouse brain. The peak brain uptake (7.5% injected dose/g tissue) was seen at 5 min post injection, followed by a gradual decline. The time-radioactivity curves showed that the highest accumulation of [¹⁸F]ASEM radioactivity occurred in the colliculus, hippocampus and frontal cortex, intermediate radioactivity was observed in the striatum and the rest of the brain and the lowest radioactivity was seen in the cerebellum. This distribution of [¹⁸F]ASEM radioactivity is comparable to the in vitro distribution of α 7-nAChRs in rodent brain tissue [65, 66].

The high α 7-nAChR specificity of [¹⁸F]ASEM binding was demonstrated by the blocking experiments in CD1 mice with the selective α 7-nAChR partial agonist SSR180711 (**Fig. 7**). For this study each animal was injected with a mixture of [¹⁸F]ASEM and SSR180711. As expected, the [¹⁸F]ASEM accumulation in the α 7-nAChR-rich brain regions was dose-dependently blocked by SSR180711. This result proved that [¹⁸F]ASEM uptake in the mouse brain is specific and mediated by α 7-nAChRs. The dose escalation blockade also demonstrated that [¹⁸F]ASEM is a suitable tool for in vivo evaluation of potential new α 7-nAChR drugs.

One of the main characteristics of PET radiotracers is binding potential (BP_{ND}), which is the ratio of specific-to-nonspecific binding [67]. Good PET tracers are expected to demonstrate $BP_{ND} > 1$. The binding potential values of [¹⁸F]ASEM in the mouse α 7-nAChR – rich regions cortex (5.3), hippocampus, (5.5) and colliculus (8.0) (Table 3)[48] were high and sufficient for the receptor quantification.

The α 7-nAChR in vivo selectivity of [¹⁸F]ASEM binding in the mouse brain was tested by the blocking experiments with several non- α 7-nAChR CNS drugs (**Fig. 8**). The drugs were ondansetron (selective 5-HT₃ antagonist), SCH23390 (D₁- and D₅-antagonist and 5-HT_{1C/2C} agonist), ketanserin (5-HT₂/5-HT_{2C} antagonist), naltrindole (selective δ -opioid antagonist), cytosine (α 4 β 2-nAChR-selective partial agonist). None of these drugs except the positive control SSR180711 reduced accumulation of [¹⁸F]ASEM radioactivity when compared to the baseline controls[48]. The absence of blockade with the α 4 β 2-nAChR-selective cytosine and 5-HT₃-selective ondansetron was especially remarkable because α 7-nAChR ligands often are not selective and bind at these receptors.

These studies in CD1 mice showed that [¹⁸F]ASEM labels α 7-nAChR receptors in the mouse brain with high degree of specificity and selectivity [48] (Figs. 6-8). In the opinion of the [¹⁸F]ASEM developers the high specific binding of this radiotracer is chiefly attributed

to its superior binding affinity versus the previous $\alpha 7$ -nAChR radiotracers. This is supported by the correlation of the binding affinity and binding potential of [^{18}F]ASEM and other radiotracers (Fig. 9).

In a parallel set of experiments the *para*-[^{18}F]ASEM was also tested in CD1 mice. The pattern of regional distribution of *para*-[^{18}F]ASEM was comparable to that of [^{18}F]ASEM. However, in agreement with its lower binding affinity *para*-[^{18}F]ASEM exhibited lower specific binding in mice than [^{18}F]ASEM (Tables 1 and 3).

4.2 Radiometabolite analysis of [^{18}F]ASEM in blood and brain

Most PET radiotracers undergo metabolism and generate various radiometabolites that, ideally, do not accumulate in the brain and spoil the quality of the PET image and thus reduce the accuracy of the quantification of the targeted receptor. Conventionally, the brain radiometabolites are considered to be insignificant for accurate quantification if the fraction of the parent radiotracer in the brain is greater than 95%.

The HPLC analysis of blood samples from CD-1 mice, and, also, from baboons[59] and human subjects[68] demonstrated that the parent compound [^{18}F]ASEM was gradually metabolized to the same hydrophilic radiometabolites in all three species. Luckily, only a small fraction of [^{18}F]ASEM radiometabolites penetrates the blood-brain barrier and the main radioactive compound in the brain is the parent [^{18}F]ASEM (>95%), as it is shown by the HPLC analysis of the mouse brain tissue. Because the radiometabolite fraction in the brain tissue is insignificant, mathematical PET modeling of the radiometabolites is not necessary for quantification of $\alpha 7$ -nAChRs with [^{18}F]ASEM [59].

4.3 Clinical $\alpha 7$ -nAChR drugs block the [^{18}F]ASEM binding in the mouse brain.

Several drugs that target $\alpha 7$ -nAChRs are now in the clinical phases of development for treatment of cognitive deficit in various pathologies [27-29]. DMXB-A was the first selective $\alpha 7$ -nAChR agonist to demonstrate cognitive enhancement and improvement in negative symptoms in patients with schizophrenia[69, 70]. The more recent drug EVP-6124 (Encenicline) is an $\alpha 7$ -nAChR selective partial agonist that is now in a number of clinical trials for treatment of Alzheimer's disease and schizophrenia (see <https://clinicaltrials.gov>). It was of interest to test the blocking effect of the clinical doses of the $\alpha 7$ -nAChR drugs in the PET experiments with [^{18}F]ASEM.

DMXB-A dose-dependently blocked the [^{18}F]ASEM binding in the $\alpha 7$ -nAChR - rich brain regions in mice (Fig. 10a)[68]. The blocking effect was significant when a clinical equivalent dose was used. This result demonstrates the potential feasibility for evaluating the effect of the clinical drug DMXB-A in human subjects with [^{18}F]ASEM, and opens new ways to study the biochemical mechanism of drugs for treatment of cognitive performance in patients with schizophrenia. In addition to DMXB-A, similar [^{18}F]ASEM blocking studies were performed with two other nicotinic drugs [68] in clinical trials that bind at $\alpha 7$ -nAChR, EVP-6124[71] and Varenicline (binds at $\alpha 4\beta 2$ - and $\alpha 7$ -nAChRs [72]) (Figs. 10b,c).

It is noteworthy, that clinical dose equivalents of $\alpha 7$ -nAChR drugs EVP-6124 and DMXB-A only partially blocked the binding of [^{18}F]ASEM in the mouse brain (23-28% and 45-55%,

respectively) (Fig. 10a,b). This degree of blockade is comparable to the currently accepted degree of $\alpha 7$ -nAChR occupancy required to achieve clinical or behavioral efficacy. The $\alpha 7$ -nAChR receptors have five binding sites distributed between five $\alpha 7$ subunits. When an agonist is applied to a population of $\alpha 7$ -nAChRs, the maximum $\alpha 7$ -nAChR receptor activation may occur when two of the five possible binding sites are occupied [73, 74]. At higher concentrations, agonists desensitize the $\alpha 7$ -nAChR and may bind to all five binding sites. In agreement with this mechanism, pre-clinical studies and clinical trials suggest that efficacious concentrations of EVP-6124 (Encenicline) is low and sufficient to occupy only one binding site on the $\alpha 7$ -nAChRs [71, 75]. It was hypothesized that endogenous acetylcholine (ACh) is required to bind to another site on the $\alpha 7$ -nAChR in order to activate the receptor channel opening. Because ACh exhibits low $\alpha 7$ -nAChRs binding affinity the complex ACh* $\alpha 7$ -nAChR quickly dissociates after the receptor channel opening and, thus, $\alpha 7$ -nAChRs are activated by low clinical doses of EVP-6124, but are not desensitized.

This mechanism of action agrees with the observed degree of [^{18}F]ASEM blockade with EVP-6124 and DMXB-A and suggests that in the future human PET studies with clinically efficacious doses of $\alpha 7$ -nAChR agonists the binding of [^{18}F]ASEM will not be blocked more than 20% - 40%.

4.4 Distribution of [^{18}F]ASEM in DISC1 mice, a rodent model of schizophrenia.

Post-mortem research demonstrated significantly lower density of $\alpha 7$ -nAChRs in the brains of schizophrenia subjects vs. controls (see Introduction for references). Mutant DISC1 mice provide a model for brain and behavioral phenotypes seen in schizophrenia [76]. Based on the favorable imaging properties identified in control CD1 mice, the [^{18}F]ASEM binding was investigated in DISC1 mice. In agreement with the reduced density of $\alpha 7$ -nAChRs in the brain tissue of schizophrenic subjects, the [^{18}F]ASEM binding in the $\alpha 7$ -nAChR – rich brain regions was significantly lower in the DISC1 mice when compared to control animals (data not shown, see paper [59]). This result emphasizes the potential utility of [^{18}F]ASEM for imaging of $\alpha 7$ -nAChRs in schizophrenia.

5. PET-[^{18}F]ASEM imaging of $\alpha 7$ -nAChRs in baboons.

The successful brain distribution studies of [^{18}F]ASEM in rodents (see above) provided a foundation for further pre-clinical evaluation in baboons [59]. The main purpose of these studies was to determine if (1) [^{18}F]ASEM exhibits the brain regional distribution that matches the distribution of $\alpha 7$ -nAChRs in non-human primates; (2) the binding is $\alpha 7$ -nAChR specific; (3) the brain pharmacokinetics of [^{18}F]ASEM are suitable for quantification of $\alpha 7$ -nAChRs and (4) to evaluate the PET imaging characteristics of [^{18}F]ASEM by mathematical modeling methods.

In PET baboon experiments [^{18}F]ASEM exhibited high and reversible brain uptake that peaked (500% standardized uptake value (%SUV)) at 20 min post injection of the radiotracer (Fig. 11) [59]. The distribution pattern of the [^{18}F]ASEM radioactivity was heterogeneous (thalamus > insula > anterior cingulate cortex > putamen > hippocampus > cortical regions > pons ~ cerebellum ~ corpus callosum) and consistent with previously published in vitro distribution of $\alpha 7$ -nAChRs in non-human primates [40, 41, 77].

The $\alpha 7$ -nAChR specificity of the [^{18}F]ASEM binding in the baboon brain was established in the blocking PET experiments. The dose-dependent blockade of [^{18}F]ASEM uptake with selective $\alpha 7$ -nAChR partial agonist SSR180711 demonstrated that the binding of [^{18}F]ASEM is mediated by $\alpha 7$ -nAChR (Fig. 12).

The baseline and blocking PET studies allowed calculation of one of the main PET imaging characteristics of [^{18}F]ASEM in baboon, the binding potential ($\text{BP}_{\text{ND}} = 3.9 - 6.6$)[59]. The value of BP_{ND} is quite high for PET and suitable for reliable quantification of $\alpha 7$ -nAChRs. For comparison, all previous $\alpha 7$ -nAChR radioligands exhibited $\text{BP}_{\text{ND}} < 1$ [35, 46-48].

6. First-in-human PET - [^{18}F]ASEM imaging of $\alpha 7$ -nAChRs[68].

Previously, the lack of a specific PET radioligand has impeded the accurate mapping and quantification of $\alpha 7$ -nAChRs in the living human brain. In the first-in-human PET studies in five healthy male subjects under an IND, [^{18}F]ASEM radioactivity peaked in the brain at 20 min after bolus injection with a robust uptake value of 400 %SUV (Fig. 13). The brain pharmacokinetics were reversible and demonstrated a decline of radioactivity concentration after the peak[68]. The highest regional brain uptake (total volume of distribution V_T , calculated with plasma reference graphic analysis) was seen in the parietal cortex ($V_T=22\pm 1.8$) ~ putamen (21.8 ± 2.9) > thalamus (20.9 ± 3.0) > cingulate (19.6 ± 2.2) > temporal lobes (19.7 ± 1.8) ~ frontal lobes (19.3 ± 1.9) > hippocampus ($V_T=17.9\pm 1.9$); moderate uptake was found in the cerebellum (15.1 ± 1.6) and brainstem (14.8 ± 1.7); and the lowest uptake was in the corpus callosum (9.9 ± 2.0). The regional distribution of [^{18}F]ASEM in the human brain matches the post-mortem human and non-human primate data [59, 78, 79]. The test-retest variability (TRV) was $10.8\pm 5.1\%$, which characterises [^{18}F]ASEM as a reproducible PET radiotracer.

7. Conclusion

In summary, during the past decade we have witnessed substantial efforts to develop a PET radioligand for quantification of $\alpha 7$ -nAChRs in the human brain. Several research groups have radiolabeled a number of $\alpha 7$ -nAChR compounds with [^{18}F] and [^{11}C] for PET. Unfortunately, these radioligands did not show suitable specific binding *in vivo* due to insufficient $\alpha 7$ -nAChR binding affinity. The recently developed [^{18}F]ASEM, a highly $\alpha 7$ -nAChR specific and selective radiotracer for brain PET, demonstrated excellent *in vivo* imaging properties in the rodents and baboons and was successfully translated to human subjects. [^{18}F]ASEM opens new horizons for studying $\alpha 7$ -nAChRs in the living human brain.

8. Acknowledgement

The author received NIH grants AG037298 and NS089437 and funds from the Department of Radiology. Special thanks to Drs. Robert Dannals, Yongjun Gao, Hayden Ravert, Dean Wong, Martin Pomper, Hiroto Kuwabara, Mikhail Pletnikov from Johns Hopkins University and Dr. Kenneth Kellar from Georgetown University for fruitful discussions and Julia Buchanan for the editorial assistance.

References

- [1]. Lukas RJ, Changeux JP, Le Novere N, Albuquerque EX, Balfour DJ, Berg DK, et al. International Union of Pharmacology. XX. Current status of the nomenclature for nicotinic acetylcholine receptors and their subunits. *Pharmacol Rev.* 1999; 51:397–401. [PubMed: 10353988]
- [2]. Philip NS, Carpenter LL, Tyrka AR, Price LH. Nicotinic acetylcholine receptors and depression: a review of the preclinical and clinical literature. *Psychopharmacology (Berl).* 2010; 212:1–12. [PubMed: 20614106]
- [3]. Ishikawa M, Hashimoto K. alpha7 nicotinic acetylcholine receptor as a potential therapeutic target for schizophrenia. *Curr Pharm Des.* 2011; 17:121–9. [PubMed: 21355839]
- [4]. Parri HR, Hernandez CM, Dineley KT. Research update: Alpha7 nicotinic acetylcholine receptor mechanisms in Alzheimer's disease. *Biochem Pharmacol.* 2011; 82:931–42. [PubMed: 21763291]
- [5]. Albuquerque EX, Pereira EF, Alkondon M, Rogers SW. Mammalian nicotinic acetylcholine receptors: from structure to function. *Physiol Rev.* 2009; 89:73–120. [PubMed: 19126755]
- [6]. Woodruff-Pak DS, Gould TJ. Neuronal nicotinic acetylcholine receptors: involvement in Alzheimer's disease and schizophrenia. *Behav Cogn Neurosci Rev.* 2002; 1:5–20. [PubMed: 17715584]
- [7]. D'Hoedt D, Bertrand D. Nicotinic acetylcholine receptors: an overview on drug discovery. *Expert Opin Ther Targets.* 2009; 13:395–411. [PubMed: 19335063]
- [8]. Hoffmeister PG, Donat CK, Schuhmann MU, Voigt C, Walter B, Nieber K, et al. Traumatic brain injury elicits similar alterations in alpha7 nicotinic receptor density in two different experimental models. *Neuromolecular Med.* 2011; 13:44–53. [PubMed: 20857232]
- [9]. Gotti C, Clementi F. Neuronal nicotinic receptors: from structure to pathology. *Prog Neurobiol.* 2004; 74:363–96. [PubMed: 15649582]
- [10]. Thomsen MS, Hansen HH, Timmerman DB, Mikkelsen JD. Cognitive improvement by activation of alpha7 nicotinic acetylcholine receptors: from animal models to human pathophysiology. *Curr Pharm Des.* 2010; 16:323–43. [PubMed: 20109142]
- [11]. Freedman R, Hall M, Adler LE, Leonard S. Evidence in postmortem brain tissue for decreased numbers of hippocampal nicotinic receptors in schizophrenia. *Biol Psychiatry.* 1995; 38:22–33. [PubMed: 7548469]
- [12]. Marutle A, Zhang X, Court J, Piggott M, Johnson M, Perry R, et al. Laminar distribution of nicotinic receptor subtypes in cortical regions in schizophrenia. *J Chem Neuroanat.* 2001; 22:115–26. [PubMed: 11470559]
- [13]. Court J, Spurden D, Lloyd S, McKeith I, Ballard C, Cairns N, et al. Neuronal nicotinic receptors in dementia with Lewy bodies and schizophrenia: alpha-bungarotoxin and nicotine binding in the thalamus. *J Neurochem.* 1999; 73:1590–7. [PubMed: 10501205]
- [14]. Martin-Ruiz CM, Haroutunian VH, Long P, Young AH, Davis KL, Perry EK, et al. Dementia rating and nicotinic receptor expression in the prefrontal cortex in schizophrenia. *Biol Psychiatry.* 2003; 54:1222–33. [PubMed: 14643090]
- [15]. Guan ZZ, Zhang X, Blennow K, Nordberg A. Decreased protein level of nicotinic receptor alpha7 subunit in the frontal cortex from schizophrenic brain. *Neuroreport.* 1999; 10:1779–82. [PubMed: 10501574]
- [16]. Mathew SV, Law AJ, Lipska BK, Davila-Garcia MI, Zamora ED, Mitkus SN, et al. Alpha7 nicotinic acetylcholine receptor mRNA expression and binding in postmortem human brain are associated with genetic variation in neuregulin 1. *Hum Mol Genet.* 2007; 16:2921–32. [PubMed: 17884806]
- [17]. Breese CR, Lee MJ, Adams CE, Sullivan B, Logel J, Gillen KM, et al. Abnormal regulation of high affinity nicotinic receptors in subjects with schizophrenia. *Neuropsychopharmacology.* 2000; 23:351–64. [PubMed: 10989262]
- [18]. Auld DS, Kornecook TJ, Bastianetto S, Quirion R. Alzheimer's disease and the basal forebrain cholinergic system: relations to beta-amyloid peptides, cognition, and treatment strategies. *Prog Neurobiol.* 2002; 68:209–45. [PubMed: 12450488]

- [19]. Sugaya K, Giacobini E, Chiappinelli VA. Nicotinic acetylcholine receptor subtypes in human frontal cortex: Changes in Alzheimer's disease. *J Neurosci Res.* 1990; 27:349. [PubMed: 2097379]
- [20]. Posadas I, Lopez-Hernandez B, Cena V. Nicotinic receptors in neurodegeneration. *Curr Neuropharmacol.* 2013; 11:298–314. [PubMed: 24179465]
- [21]. Thomsen MS, Weyn A, Mikkelsen JD. Hippocampal alpha7 nicotinic acetylcholine receptor levels in patients with schizophrenia, bipolar disorder, or major depressive disorder. *Bipolar Disord.* 2011; 13:701–7. [PubMed: 22085484]
- [22]. Besson VC. Drug targets for traumatic brain injury from poly(ADP-ribose)polymerase pathway modulation. *Br J Pharmacol.* 2009; 157:695–704. [PubMed: 19371326]
- [23]. Faul, M.; Xu, L.; Wald, MM.; Coronado, VG. *Traumatic Brain Injuries in the United States: Emergency Department Visits, Hospitalizations and Deaths 2002–2006.* Centers for Disease Control and Prevention, National Center for Injury Prevention and Control; Atlanta, GA: 2010.
- [24]. Verbois SL, Sullivan PG, Scheff SW, Pauly JR. Traumatic brain injury reduces hippocampal alpha7 nicotinic cholinergic receptor binding. *J Neurotrauma.* 2000; 17:1001–11. [PubMed: 11101204]
- [25]. Verbois SL, Scheff SW, Pauly JR. Time-dependent changes in rat brain cholinergic receptor expression after experimental brain injury. *J Neurotrauma.* 2002; 19:1569–85. [PubMed: 12542858]
- [26]. Kelso ML, Wehner JM, Collins AC, Scheff SW, Pauly JR. The pathophysiology of traumatic brain injury in alpha7 nicotinic cholinergic receptor knockout mice. *Brain Res.* 2006; 1083:204–10. [PubMed: 16545784]
- [27]. Mazurov AA, Speake JD, Yohannes D. Discovery and development of alpha7 nicotinic acetylcholine receptor modulators. *J Med Chem.* 2011; 54:7943–61. [PubMed: 21919481]
- [28]. Taly A, Charon S. alpha7 nicotinic acetylcholine receptors: a therapeutic target in the structure era. *Curr Drug Targets.* 2012; 13:695–706. [PubMed: 22300037]
- [29]. Wallace TL, Bertrand D. Alpha7 neuronal nicotinic receptors as a drug target in schizophrenia. *Expert Opin Ther Tar.* 2013; 17:139–55.
- [30]. Lippiello PM, Bencherif M, Hauser TA, Jordan KG, Letchworth SR, Mazurov AA. Nicotinic receptors as targets for therapeutic discovery. *Expert Opinion on Drug Discovery.* 2007; 2:1185–203. [PubMed: 23496128]
- [31]. Kem WR. The brain alpha7 nicotinic receptor may be an important therapeutic target for the treatment of Alzheimer's disease: studies with DMXBA (GTS-21). *Behav Brain Res.* 2000; 113:169–81. [PubMed: 10942043]
- [32]. Gatson JW, Simpkins JW, Uteshev VV. High therapeutic potential of positive allosteric modulation of alpha7 nAChRs in a rat model of traumatic brain injury: proof-of-concept. *Brain Res Bull.* 2015; 112:35–41. [PubMed: 25647232]
- [33]. Alavi A, Basu S. Planar and SPECT imaging in the era of PET and PET-CT: can it survive the test of time? *Eur J Nucl Med Mol Imaging.* 2008; 35:1554–9. [PubMed: 18594816]
- [34]. Rahmim A, Zaidi H. PET versus SPECT: strengths, limitations and challenges. *Nucl Med Commun.* 2008; 29:193–207. [PubMed: 18349789]
- [35]. Horti AG, Villemagne VL. The quest for Eldorado: development of radioligands for in vivo imaging of nicotinic acetylcholine receptors in human brain. *Curr Pharm Des.* 2006; 12:3877–900. [PubMed: 17073685]
- [36]. Piel M, Vernaleken I, Rosch F. Positron emission tomography in CNS drug discovery and drug monitoring. *J Med Chem.* 2014; 57:9232–58. [PubMed: 25144329]
- [37]. Halldin C, Gulyas B, Langer O, Farde L. Brain radioligands--state of the art and new trends. *Q J Nucl Med.* 2001; 45:139–52. [PubMed: 11476163]
- [38]. Eckelman WC, Reba RC, Gibson RE. Receptor-binding radiotracers: A class of potential radiopharmaceuticals. *J Nucl Med.* 1979; 20:350–7. [PubMed: 43884]
- [39]. Eckelman WC, Kilbourn MR, Mathis CA. Discussion of targeting proteins in vivo: in vitro guidelines. *Nucl Med Biol.* 2006; 33:449–51. [PubMed: 16720235]

- [40]. Kulak JM, Schneider JS. Differences in alpha7 nicotinic acetylcholine receptor binding in motor symptomatic and asymptomatic MPTP-treated monkeys. *Brain Res.* 2004; 999:193–202. [PubMed: 14759498]
- [41]. Kulak JM, Carroll FI, Schneider JS. [125I]Iodomethyllycaconitine binds to alpha7 nicotinic acetylcholine receptors in monkey brain. *Eur J Neurosci.* 2006; 23:2604–10. [PubMed: 16817863]
- [42]. Horti AG, Gao Y, Kuwabara H, Dannals RF. Development of radioligands with optimized imaging properties for quantification of nicotinic acetylcholine receptors by positron emission tomography. *Life Sci.* 2009 doi:10.1016/j.lfs.2009.02.029.
- [43]. Horti AG, Wong DF. Clinical Perspective and Recent Development of PET Radioligands for Imaging Cerebral Nicotinic Acetylcholine Receptors. *PET Clin.* 2009; 4:89–100. [PubMed: 20046884]
- [44]. Dolle F, Valette H, Hinnen F, Vaufrey F, Demphel S, Coulon C, et al. Synthesis and preliminary evaluation of a carbon-11-labelled agonist of the $\alpha 7$ nicotinic acetylcholine receptor. *J Label Compd Radiopharm.* 2001; 44:785–95.
- [45]. Pomper MG, Phillips E, Fan H, McCarthy DJ, Keith RA, Gordon JC, et al. Synthesis and biodistribution of radiolabeled alpha 7 nicotinic acetylcholine receptor ligands. *J Nucl Med.* 2005; 46:326–34. [PubMed: 15695794]
- [46]. Toyohara J, Wu J, Hashimoto K. Recent development of radioligands for imaging alpha7 nicotinic acetylcholine receptors in the brain. *Curr Top Med Chem.* 2010; 10:1544–57. [PubMed: 20583992]
- [47]. Brust, P.; Deuther-Conrad, W. Molecular imaging of alpha7 nicotinic acetylcholine receptors in vivo: current status and perspectives. In: Bright, P., editor. *Neuroimaging - Clinical Applications.* InTech; Rijeka: 2012. p. 533-58.
- [48]. Gao Y, Kellar KJ, Yasuda RP, Tran T, Xiao Y, Dannals RF, et al. Derivatives of Dibenzothiophene for Positron Emission Tomography Imaging of alpha7-Nicotinic Acetylcholine Receptors. *J Med Chem.* 2013; 56:7574–89. [PubMed: 24050653]
- [49]. Toyohara J, Sakata M, Wu J, Ishikawa M, Oda K, Ishii K, et al. Preclinical and the first clinical studies on [11C]CHIBA-1001 for mapping alpha7 nicotinic receptors by positron emission tomography. *Ann Nucl Med.* 2009; 23:301–9. [PubMed: 19337782]
- [50]. Ishikawa M, Sakata M, Toyohara J, Oda K, Ishii K, Wu J, et al. Occupancy of alpha7 Nicotinic Acetylcholine Receptors in the Brain by Tropisetron: A Positron Emission Tomography Study Using [(11)C]CHIBA-1001 in Healthy Human Subjects. *Clinical psychopharmacology and neuroscience : the official scientific journal of the Korean College of Neuropsychopharmacology.* 2011; 9:111–6. [PubMed: 23430308]
- [51]. Tanibuchi Y, Wu J, Toyohara J, Fujita Y, Iyo M, Hashimoto K. Characterization of [(3)H]CHIBA-1001 binding to alpha7 nicotinic acetylcholine receptors in the brain from rat, monkey, and human. *Brain Res.* 2010; 1348:200–8. [PubMed: 20537987]
- [52]. Ding M, Ghanekar S, Elmore CS, Zysk JR, Werkheiser JL, Lee CM, et al. [³H]Chiba-1001 (methyl-SSR180711) has low in vitro binding affinity and poor in vivo selectivity to nicotinic alpha-7 receptor in rodent brain. *Synapse.* 2012; 66:315–22. [PubMed: 22108786]
- [53]. Ravert HT, Dorff P, Foss CA, Mease RC, Fan H, Holmquist CR, et al. Radiochemical synthesis and in vivo evaluation of [18F]AZ11637326: An agonist probe for the alpha7 nicotinic acetylcholine receptor. *Nucl Med Biol.* 2013; 40:731–9. [PubMed: 23680470]
- [54]. Maier DL, Hill G, Ding M, Tuke D, Einstein E, Gurley D, et al. Pre-clinical validation of a novel alpha-7 nicotinic receptor radiotracer, [3H]AZ11637326: target localization, biodistribution and ligand occupancy in the rat brain. *Neuropharmacology.* 2011; 61:161–71. [PubMed: 21497612]
- [55]. Ettrup A, Mikkelsen JD, Lehel S, Madsen J, Nielsen EO, Palner M, et al. 11C-NS14492 as a novel PET radioligand for imaging cerebral alpha7 nicotinic acetylcholine receptors: in vivo evaluation and drug occupancy measurements. *J Nucl Med.* 2011; 52:1449–56. [PubMed: 21828113]
- [56]. Deuther-Conrad W, Fischer S, Hiller A, Becker G, Cumming P, Xiong G, et al. Assessment of alpha7 nicotinic acetylcholine receptor availability in juvenile pig brain with [18F]NS10743. *Eur J Nucl Med Mol Imaging.* 2011; 38:1541–9. [PubMed: 21484373]

- [57]. Deuther-Conrad W, Fischer S, Hiller A, Nielsen EO, Timmermann DB, Steinbach J, et al. Molecular imaging of alpha7 nicotinic acetylcholine receptors: design and evaluation of the potent radioligand [18F]NS10743. *Eur J Nucl Med Mol Imaging*. 2009; 36:791–800. [PubMed: 19137292]
- [58]. Horti AG, Ravert HT, Gao YJ, Holt DP, Bunnelle WH, Schrimpf MR, et al. Synthesis and evaluation of new radioligands [C-11]A-833834 and [C-11]A-752274 for positron-emission tomography of alpha 7-nicotinic acetylcholine receptors. *Nucl Med Biol*. 2013; 40:395–402. [PubMed: 23294899]
- [59]. Horti AG, Gao Y, Kuwabara H, Wang Y, Abazyan S, Yasuda RP, et al. [18F]ASEM ([18F]JHU82132), a radiolabeled antagonist for imaging the $\alpha 7$ -nicotinic acetylcholine receptor ($\alpha 7$ -nAChR) with positron emission tomography (PET). *J Nucl Med*. 2014; 55:672–7. [PubMed: 24556591]
- [60]. Schrimpf MR, Sippy KB, Briggs CA, Anderson DJ, Li T, Ji J, et al. SAR of alpha7 nicotinic receptor agonists derived from tilorone: exploration of a novel nicotinic pharmacophore. *Bioorg Med Chem Lett*. 2012; 22:1633–8. [PubMed: 22281189]
- [61]. Horti, AG.; Raymont, V.; Terry, GE. PET imaging of endocannabinoid system. In: Dierckx, R.; Otte, A.; De Vries, EF.; Van Waarde, A., editors. *PET and SPECT of Neurobiological Systems*. Springer; Berlin-Heidelberg: 2014. p. 251-319.
- [62]. Waterhouse RN. Determination of lipophilicity and its use as a predictor of blood-brain barrier penetration of molecular imaging agents. *Mol Imaging Biol*. 2003; 5:376–89. [PubMed: 14667492]
- [63]. Dannals, RF.; Ravert, HT.; Wilson, AA.; Wagner, HN. Special Problems Associated with the Synthesis of High Specific Activity Carbon-11 Labeled Radiotracers. In: A.M. E, editor. *New Trends Radiopharm Synthesis, Quality Assurance and Regulatory Control*. Springer US; 1991. p. 21-30.
- [64]. Ravert HT, Holt DP, Gao Y, Horti AG, Dannals RF. Microwave-assisted radiosynthesis of [(18)F]ASEM, a radiolabeled alpha7-nicotinic acetylcholine receptor antagonist. *J Labelled Comp Radiopharm*. 2015; 58:180–2. [PubMed: 25720955]
- [65]. Clarke PB, Schwartz RD, Paul SM, Pert CB, Pert A. Nicotinic binding in rat brain: autoradiographic comparison of [3H]acetylcholine, [3H]nicotine, and [125I]-alpha-bungarotoxin. *J Neurosci*. 1985; 5:1307–15. [PubMed: 3998824]
- [66]. Whiteaker P, Davies AR, Marks MJ, Blagbrough IS, Potter BV, Wolstenholme AJ, et al. An autoradiographic study of the distribution of binding sites for the novel alpha7-selective nicotinic radioligand [3H]-methyllycaconitine in the mouse brain. *Eur J Neurosci*. 1999; 11:2689–96. [PubMed: 10457165]
- [67]. Innis RB, Cunningham VJ, Delforge J, Fujita M, Gjedde A, Gunn RN, et al. Consensus nomenclature for in vivo imaging of reversibly binding radioligands. *J Cereb Blood Flow Metab*. 2007; 27:1533–9. [PubMed: 17519979]
- [68]. Wong DF, Kuwabara H, Pomper M, Holt DP, Brasic JR, George N, et al. Human Brain Imaging of Alpha-7 nAChR with [18F]ASEM: a New PET Radiotracer for Neuropsychiatry and Determination of Drug Occupancy. *Molecular Imaging and Biology*. 2014; 16:730–8. [PubMed: 25145965]
- [69]. Freedman R, Olincy A, Buchanan RW, Harris JG, Gold JM, Johnson L, et al. Initial phase 2 trial of a nicotinic agonist in schizophrenia. *Am J Psychiatry*. 2008; 165:1040–7. [PubMed: 18381905]
- [70]. Olincy A, Harris JG, Johnson LL, Pender V, Kongs S, Allensworth D, et al. Proof-of-concept trial of an alpha7 nicotinic agonist in schizophrenia. *Arch Gen Psychiatry*. 2006; 63:630–8. [PubMed: 16754836]
- [71]. Prickaerts J, van Goethem NP, Chesworth R, Shapiro G, Boess FG, Methfessel C, et al. EVP-6124, a novel and selective alpha7 nicotinic acetylcholine receptor partial agonist, improves memory performance by potentiating the acetylcholine response of alpha7 nicotinic acetylcholine receptors. *Neuropharmacology*. 2012; 62:1099–110. [PubMed: 22085888]
- [72]. Rollema H, Shrikhande A, Ward KM, Tingley FD 3rd, Coe JW, O'Neill BT, et al. Pre-clinical properties of the alpha4beta2 nicotinic acetylcholine receptor partial agonists varenicline,

- cytisine and dianicline translate to clinical efficacy for nicotine dependence. *Br J Pharmacol.* 2010; 160:334–45. [PubMed: 20331614]
- [73]. Williams DK, Wang J, Papke RL. Investigation of the molecular mechanism of the alpha7 nicotinic acetylcholine receptor positive allosteric modulator PNU-120596 provides evidence for two distinct desensitized states. *Mol Pharmacol.* 2011; 80:1013–32. [PubMed: 21885620]
- [74]. Papke RL. Merging old and new perspectives on nicotinic acetylcholine receptors. *Biochem Pharmacol.* 2014; 89:1–11. [PubMed: 24486571]
- [75]. Preskorn SH, Gawryl M, Dgetluck N, Palfreyman M, Bauer LO, Hilt DC. Normalizing effects of EVP-6124, an alpha-7 nicotinic partial agonist, on event-related potentials and cognition: a proof of concept, randomized trial in patients with schizophrenia. *Journal of psychiatric practice.* 2014; 20:12–24. [PubMed: 24419307]
- [76]. Pletnikov MV, Ayhan Y, Nikolskaia O, Xu Y, Ovanesov MV, Huang H, et al. Inducible expression of mutant human DISC1 in mice is associated with brain and behavioral abnormalities reminiscent of schizophrenia. *Mol Psychiatry.* 2008; 13:173–86. [PubMed: 17848917]
- [77]. Han ZY, Zoli M, Cardona A, Bourgeois JP, Changeux JP, Le Novère N. Localization of [3H]nicotine, [3H]cytisine, [3H]epibatidine, and [125I]alpha-bungarotoxin binding sites in the brain of *Macaca mulatta*. *J Comp Neurol.* 2003; 461:49–60. [PubMed: 12722104]
- [78]. Court JA, Martin-Ruiz C, Graham A, Perry E. Nicotinic receptors in human brain: topography and pathology. *J Chem Neuroanat.* 2000; 20:281–98. [PubMed: 11207426]
- [79]. Breese CR, Adams C, Logel J, Drebing C, Rollins Y, Barnhart M, et al. Comparison of the regional expression of nicotinic acetylcholine receptor alpha7 mRNA and [125I]-alpha-bungarotoxin binding in human postmortem brain. *J Comp Neurol.* 1997; 387:385–98. [PubMed: 9335422]
- [80]. Xiao Y, Kellar K. The comparative pharmacology and up-regulation of rat neuronal nicotinic receptor subtype binding sites stably expressed in transfected mammalian cells. *J Pharmacol Exp Ther.* 2004; 310:98–107. [PubMed: 15016836]
- [81]. Reagan-Shaw S, Nihal M, Ahmad N. Dose translation from animal to human studies revisited. *FASEB J.* 2008; 22:659–61. [PubMed: 17942826]

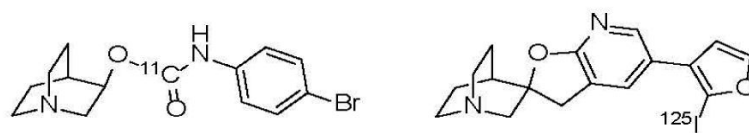


Fig. 1.
First radioligands for emission tomography imaging of $\alpha 7$ -nAChR [44, 45].

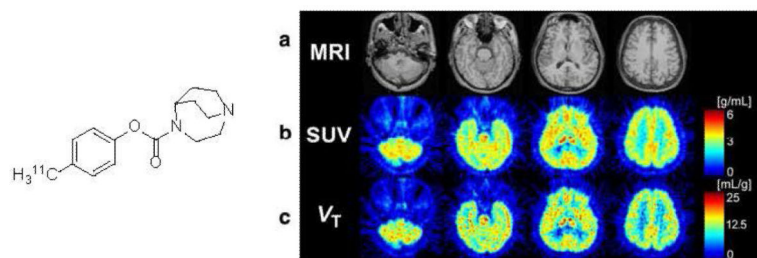


Fig. 2.

Left: Structure of $[^{11}\text{C}]\text{CHIBA-1001}$. **Right:** PET images of human brain with $[^{11}\text{C}]\text{CHIBA-1001}$. Panel **a** Magnetic resonance images (MRI) of the corresponding slices. Panel **b** Static images acquired from 0 to 90 min after injection of $[^{11}\text{C}]\text{CHIBA-1001}$ expressed as SUV. Panel **c** A parametric image for the total distribution volume of $[^{11}\text{C}]\text{CHIBA-1001}$ generated using Logan graphical analysis. The data from 30 to 90 min were applied to the Logan plot analysis. Reprinted from [49] with permission of Copyright Clearance Center's RightsLink service.

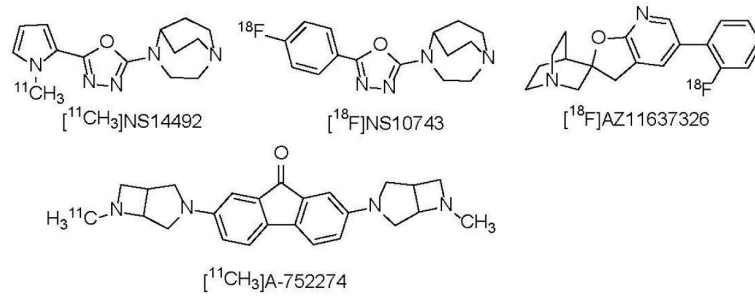


Fig. 3. Recent $\alpha 7$ -nAChR PET radioligands, $[^{18}\text{F}]\text{AZ11637326}$ [53, 54], $[^{11}\text{C}]\text{NS14492}$ [55], $[^{18}\text{F}]\text{NS10743}$ [56, 57] and $[^{11}\text{C}]\text{A-752274}$ [58].

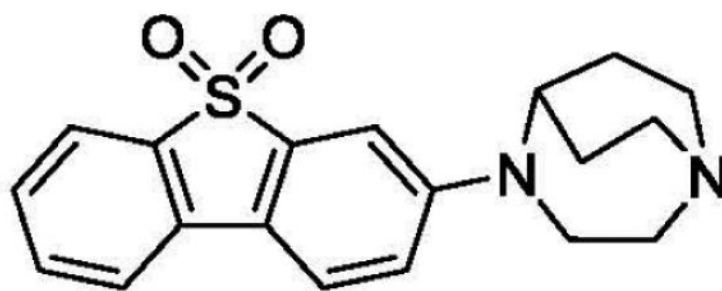


Fig. 4. Structure of 3-(1,4-diazabicyclo[3.2.2]nonan-4-yl)dibenzo[*b,d*]thiophene 5,5-dioxide, an α 7-nAChR selective ligand with high binding affinity that was developed by Abbott[60].

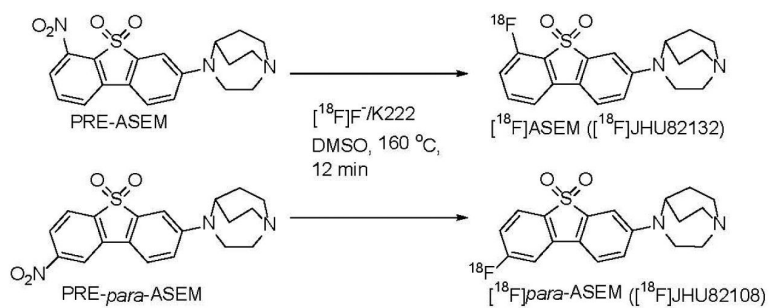


Fig. 5. Radiosynthesis of ^{18}F ASEM and *para*- ^{18}F ASEM using a PC-controlled radiochemistry synthesis module (Microlab, GE) [48].

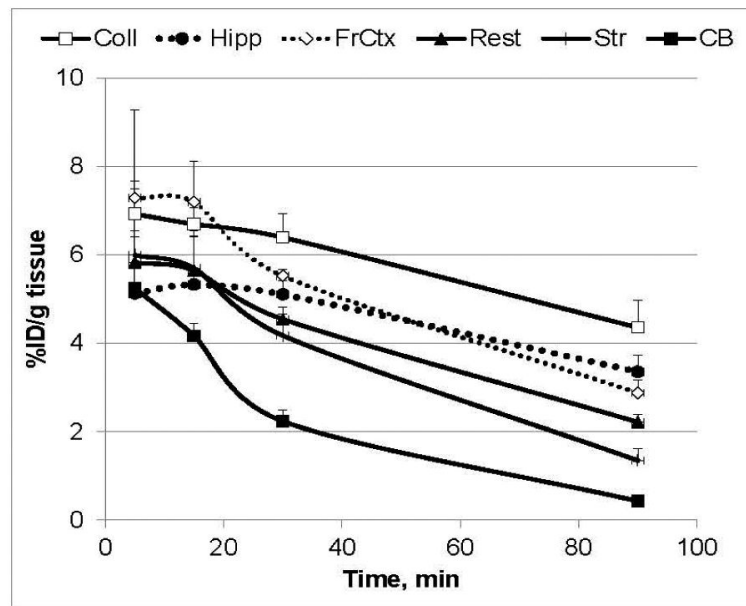


Fig. 6. Regional distribution of [^{18}F]ASEM in CD-1 mice. Data: mean % injected dose/g tissue \pm SD (n = 3). Abbreviations: Coll = superior and inferior colliculus; Hipp = hippocampus; FrCtx = frontal cortex; Rest = rest of brain; Str = striatum; CB = cerebellum. Reprinted from [48] with permission of Copyright Clearance Center's RightsLink service. The study demonstrated that [^{18}F]ASEM exhibits high brain uptake with regional distribution that matches the distribution of the $\alpha 7$ -nAChR in the rodent brain and reversible brain kinetics.

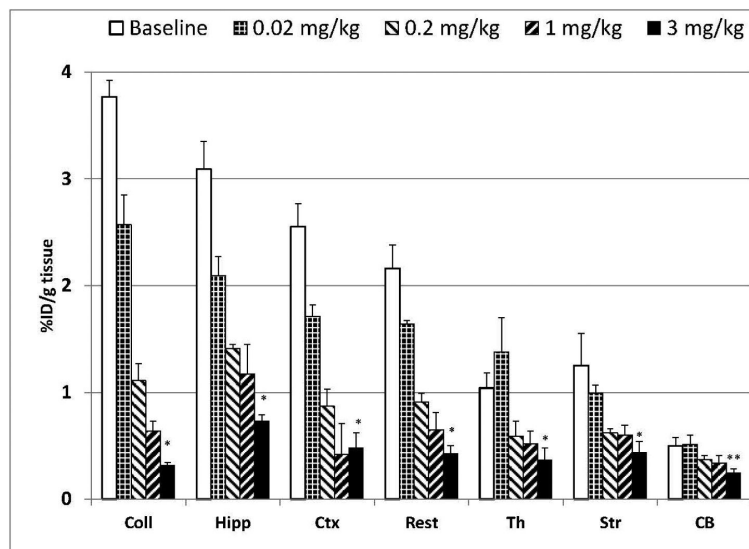


Fig. 7. Dose dependent blockade of [^{18}F]ASEM (0.07 mCi, specific radioactivity = 7900 mCi/ μmol , i.v.) accumulation by intravenous co-injection of SSR180711, a selective $\alpha 7$ -nAChR partial agonist (doses 0.02 mg/kg, 0.2 mg/kg, 1 mg/kg, 3 mg/kg) in the CD-1 mouse brain regions 90 min after the injection. * $P < 0.01$, significantly different from controls (ANOVA). Data: mean %injected dose/g tissue \pm SD (n=3). Abbreviations: Coll = superior and inferior colliculus; Hipp = hippocampus; Ctx = cortex; Str = striatum; Th = thalamus; Rest = rest of brain; CB = cerebellum. Reprinted from [48] with permission of Copyright Clearance Center's RightsLink service

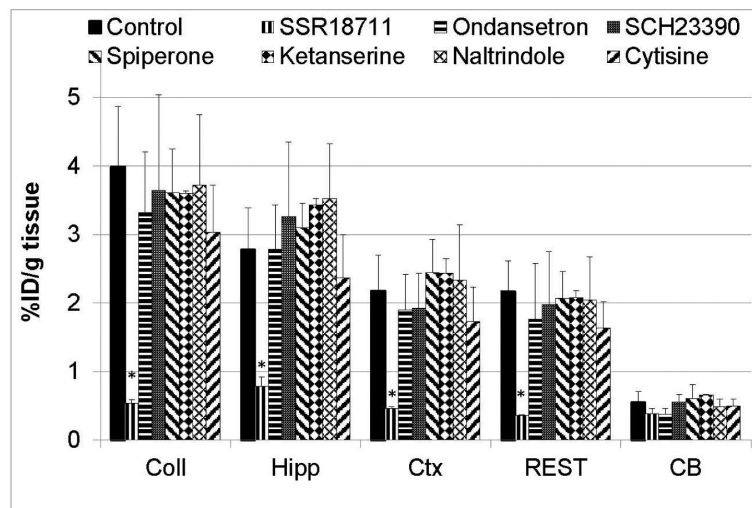


Fig. 8.

Effect of various CNS drugs (2 mg/kg, s.c.) on accumulation of [^{18}F]ASEM in CD-1 mouse brain regions 90 min after injection of tracer expressed as %ID/g tissue. Abbreviations: Coll = superior and inferior colliculus; Hipp = hippocampus; Ctx = cortex; CB = cerebellum; REST = rest of brain. Data are mean \pm SD (n=3). * $P < 0.01$, significantly different from controls ($P > 0.01$) (ANOVA, single-factor analysis). The graph demonstrates that unlike the positive control (SSR180711) all non- $\alpha 7$ -nAChR CNS drugs do not have an effect on the cerebral uptake of [^{18}F]ASEM that is $\alpha 7$ -nAChR selective in vivo. Drugs: SSR180711 – selective $\alpha 7$ -nAChR partial agonist; Ondansetron - selective 5-HT $_3$ antagonist; SCH23390 -D $_1$ - and D $_5$ -antagonist and 5-HT $_{1C/2C}$ agonist; Ketanserin - 5-HT $_2/5$ -HT $_{2C}$ antagonist; Naltrindole - Selective δ -opioid antagonist; Cytisine – $\alpha 4\beta 2$ -nAChR agonist [48].

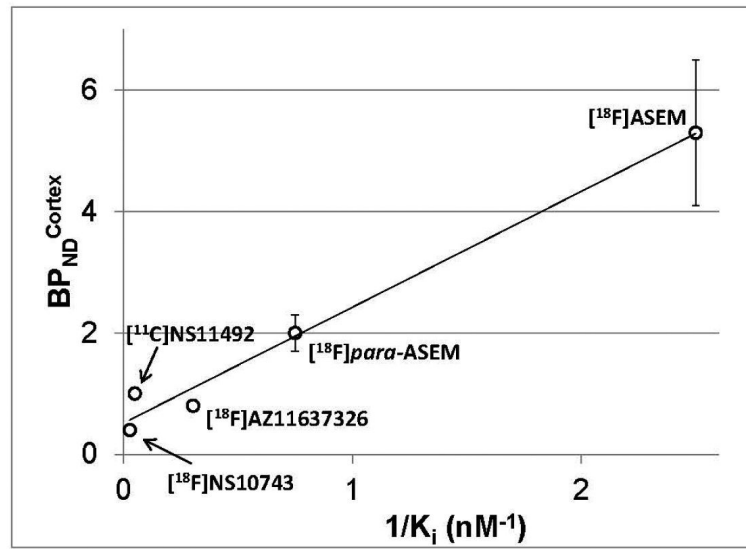


Fig. 9. Correlation of the BP_{ND}^{cortex} (unitless) vs. $1/K_i (nM^{-1})$ of $\alpha 7$ -nAChR PET radioligands $[^{18}F]AZ11637326$, $[^{11}C]NS14492$, $[^{18}F]NS10743$, $[^{18}F]para-ASEM$ and $[^{18}F]ASEM$ ($y = 1.91x + 0.52$, $R^2 = 0.98$). All K_i values were obtained under the same binding assay conditions. Reprinted from [48] with permission of Copyright Clearance Center's RightsLink service

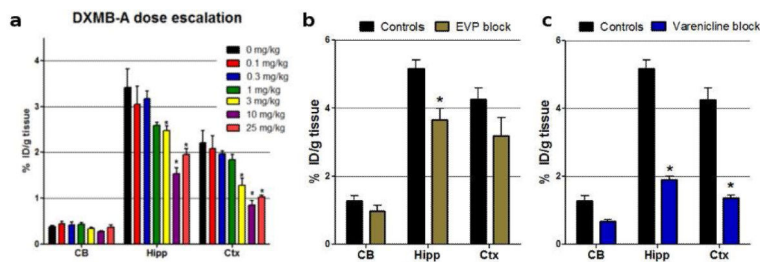


Fig. 10.

Baseline versus blockade studies of [^{18}F]ASEM with mouse-equivalent doses of clinical $\alpha 7$ -nAChR drugs in CD-1 mice. Data: %ID/g tissue \pm SD (n = 4). The control mice were treated with vehicle saline. Abbreviations: CB = cerebellum, Hipp = hippocampus; Ctx = cortex. Statistics in all three graphs: *P < 0.01, blockade is significantly different from controls (ANOVA). **a:** DMXB-A (GTS-21), dose-escalation. Note: a mouse-equivalent dose = 25 mg/kg[81] of the clinical dose (150 mg). 90 min post [^{18}F]ASEM injection. **b:** EVP-6124, a mouse-equivalent dose (0.18 mg/kg) of the clinical dose (1 mg). 60 min post [^{18}F]ASEM injection. **c:** Varenicline, a mouse-equivalent dose (0.18 mg/kg) of the clinical dose (1 mg). 60 min post [^{18}F]ASEM injection. The graph demonstrates that in vivo binding of [^{18}F]ASEM in the mouse brain regions enriched with $\alpha 7$ -nAChR is significantly blocked by the $\alpha 7$ -nAChR drugs DMXB-A, EVP-6124 and varenicline. Reprinted from[68] with permission of Copyright Clearance Center's RightsLink service.

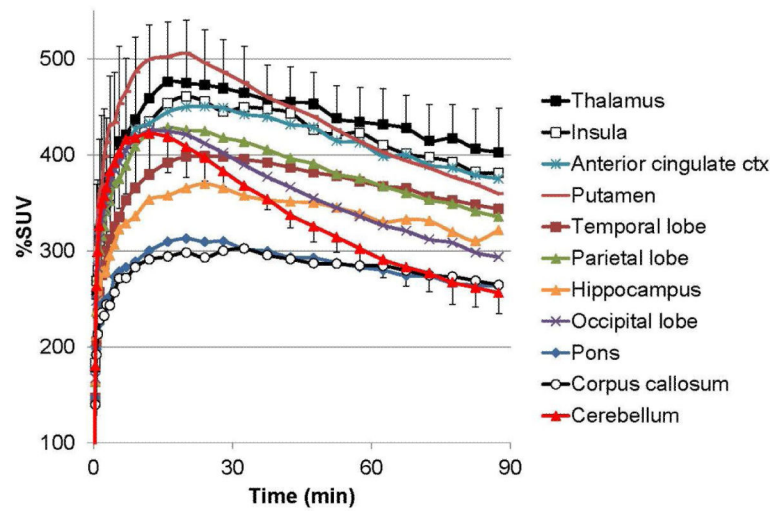


Fig. 11. Baseline cerebral time-activity curves (TACs) after bolus administration of [^{18}F]ASEM in three baboons. The graph demonstrates a substantial heterogeneous brain uptake of [^{18}F]ASEM that matches the distribution of $\alpha 7$ -nAChR in non-human primates [40, 41, 77] and reversible brain kinetics. Data: mean Standardized Uptake Values (%SUV) \pm SD (n = 3). Reprinted from [59] with permission of SNMMI.

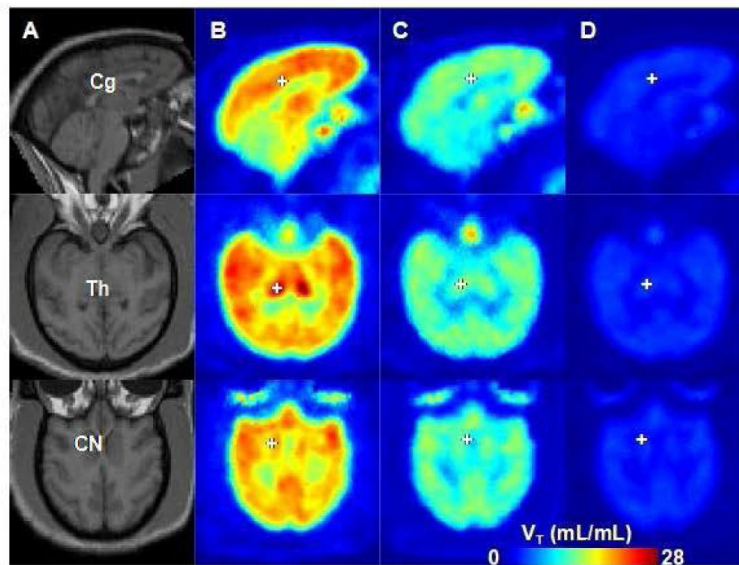


Fig. 12. Sagittal (Top row), and trans-axial (Middle and Bottom rows) views of V_T images of [^{18}F]ASEM in the same baboon for a baseline PET scan (B), and after administration of 0.5 mg/kg (C) and 5 mg/kg (D) of SSR180711, a selective $\alpha 7$ -nAChR partial agonist. MR images (A) indicate locations of selected brain structures including the cingulate cortex (Cg), thalamus (Th), and caudate nucleus (CN), which are indicated by + in the V_T images (D). The V_T images are displayed using the same minimum and maximum values for all scanning conditions. These data demonstrate the dose dependent blockade of [^{18}F]ASEM in baboon brain and provide evidence that [^{18}F]ASEM is specific and mediated by $\alpha 7$ -nAChR. The images also suggest that there is no reference region devoid of $\alpha 7$ -nAChRs. Reprinted from [59] with permission of SNMMI.

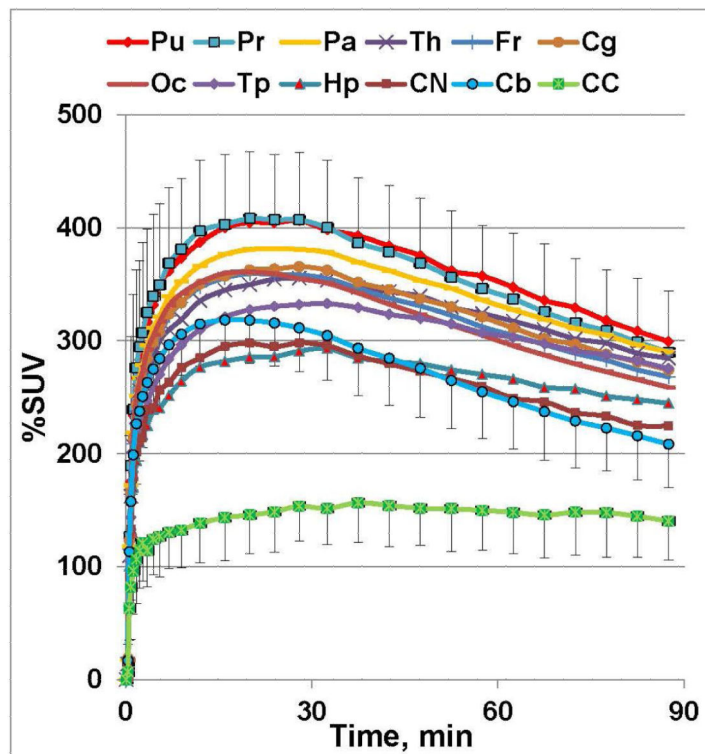


Fig. 13.

Baseline PET/ ^{18}F]ASEM TAC's (%SUV \pm SD (n = 5)) in healthy human males.

Abbreviations: Pu = putamen; Pr = precuneous; Pa = parietal lobe; Th = thalamus; Fr = frontal lobe; Cg = cingulate; Oc = occipital; Tp = temporal lobe; Hp = hippocampus; CN = caudate nucleus; Cb = cerebellum; CC = corpus callosum. The distribution of ^{18}F]ASEM in the human brain regions is comparable with non-human primate (see for review [34]) and human post-mortem distribution of $\alpha 7$ -nAChR [47-48]. The brain kinetics of ^{18}F]ASEM are reversible. Reprinted from [68] with permission of Copyright Clearance Center's RightsLink service.

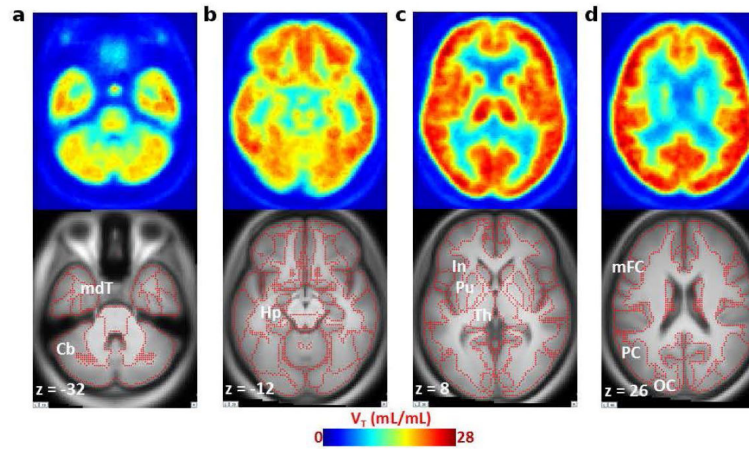
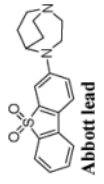
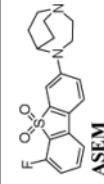
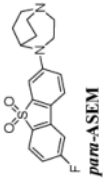


Fig. 14.

Averaged ($n = 5$) transaxial images of a spatially normalized V_T map of [^{18}F]ASEM and matching MRI in healthy control subjects. Cerebellum (Cb) and medial temporal cortex (mdT; panel **a**) show relatively low V_T values and hippocampus (Hp; panel **b**) show medium V_T values. The insula (In), putamen (Pu), and thalamus (Th) are shown in panel **c**, and middle frontal (mFC), parietal (PC), and occipital (OC) cortices (panel **d**) exhibit high V_T values in the human brain. Red dots on MRI images indicate outlines of cortical and subcortical structures. Reprinted from [68] with permission of Copyright Clearance Center's RightsLink service.

Inhibition in vitro binding affinities (K_i , nM) of ASEM, para-ASEM and the Abbott lead toward $\alpha 7$ -nAChR, heteromeric nAChR subtypes and 5-HT₃ [48].

Table 1

Compound	$\alpha 7$ -nAChR ^a	Heteromeric nAChR subtypes ^b					5-HT ₃ ^c	Selectivity	
		$\alpha 2\beta 2$	$\alpha 3\beta 4$	$\alpha 3\beta 2$	$\alpha 3\beta 4$	$\alpha 4\beta 2$		$\alpha 4\beta 4$	$\alpha 7/\alpha 4\beta 2$
 Abbott lead	0.3, 0.5	-	-	-	-	-	660 ^d	-	-
 ASEM (JHU82132)	0.37, 0.45	>10000	4000	1000	709	562	230	1370	561
 para-ASEM (JHU82108)	1.32, 1.35	1000	8000	2000	5000	885	505	663	378

^aRat cortical membranes, radiotracer [¹²⁵I]α-bungarotoxin (0.1 nM), $K_D = 0.7$ nM

^bInhibition in vitro binding assay of all heteromeric nAChR subtypes was performed with stably transfected HEK293 cells and [³H]lepipatidine (0.5 nM), $K_D = 0.021$ nM (α2β2-nAChR), $K_D = 0.084$ nM (α2β4-nAChR), $K_D = 0.034$ nM (α3β2-nAChR), $K_D = 0.29$ nM (α3β4-nAChR), $K_D = 0.046$ nM (α4β2-nAChR), $K_D = 0.094$ nM (α4β4-nAChR).[80]

^cHuman 5-HT₃ recombinant/HEK293 cells, radiotracer [³H]GR65630 (0.35 nM), $K_D = 0.5$ nM

^dthe K_i value is taken from[60]

Table 2

Comparison of in vitro $\alpha 7$ -nAChR inhibition binding affinities of ASEM versus previous PET radioligands NS14492, NS10743, AZ11637326.

Compound	K_i , nM ^a [48]
NS14492	20.4
NS10743	38.0
AZ11637326	3.3
ASEM	0.37, 0.45

^aThe binding assay performed under the same conditions: rat cortical membranes, radiotracer [¹²⁵I] α -bungarotoxin (0.1 nM), K_D = 0.7 nM (commercial assay, CEREP, www.cerep.fr).

Author Manuscript

Author Manuscript

Author Manuscript

Author Manuscript

Table 3

Approximate binding potential (BP_{ND}) values (unitless) of [¹⁸F]ASEM and *para*-[¹⁸F]ASEM in the mouse brain regions. Data: mean ± SD (n = 6) [48].

Compound	Region	Superior & inferior colliculus	Hippocampus	Cortex
[¹⁸ F]ASEM		8.0 ± 1.6	5.5 ± 1.7	5.3 ± 1.2
<i>para</i> -[¹⁸ F]ASEM		2.0 ± 0.5	3.1 ± 0.7	2.0 ± 0.3